

Distributed Voltage Regulation in Distribution Power Grids: Utilizing the Photovoltaics Inverters

Chenye Wu, Gabriela Hug, and Soumya Kar

Abstract—Millions of newly installed photovoltaic (PV) panels are disrupting the conventional distribution power grid operation. The lack of efficient coordination schemes between the PV panels results in voltage stability issues. In this paper, we exploit the reactive power control potential in the inverters of the PV panels for voltage regulation. There are considerable obstacles to design a coordination scheme that does not rely on a central entity with theoretical performance guarantee. In particular, the power flow equations define a highly non-convex constraint set. To tackle this challenge, we first examine the structure of the problem for a simplified linear network model, which allows for the design of a distributed control scheme. Then, we devise an analytical framework to show that our proposed distributed scheme will converge to a local minimum geometrically in the non-convex branch flow model. We further characterize the systematic error during the convergence. Finally, we use simulations to assess the performance of our proposed scheme.

I. INTRODUCTION

Pressing environmental problems drive the world-wide interest in renewable energy. In addition, nuclear power safety concerns, such as in Germany where the goal is to have no operational nuclear plants by 2020 [1], help accelerate the adoption of renewables. Investment in renewables today is mostly in utility-scale solar and wind plants, as well as small-scale distributed rooftop photovoltaics (PV).

A. Opportunities and Challenges

The newly installed rooftop PV panels, however, have posed several existential threats to the distribution system operation, among which, the most critical one is the voltage stability issue [3]. The challenge with respect to the voltage profiles is twofold. First, the conventional distribution grid lacks voltage control and local measurement units. This situation has been changed dramatically over the past decades with the blossom of smart grid initiatives. Increasing distributed generation units with voltage control potentials and phasor measurement units (PMUs) are being deployed in the distribution grids across the world. The second challenge, which is more critical, is the lack of an efficient coordination scheme to utilize the potential of the new components. Our paper is targeting this second challenge. We utilize the capability of the PV inverters to provide flexible reactive power for voltage regulation. Our focus is on coordinating all the PV panels to achieve the desired voltage profile in the

distribution grid. To avoid the need for a centralized control entity, a distributed control scheme is proposed.

B. Related Works

One major body of related literature on distributed voltage regulation scheme investigates the resource coordination and scheduling. The power flow equations in the distribution network render the optimization or the control problem non-convex. Most works rely on linearizing the power flow equations around the operating point and then conduct the voltage regulation, including [4], [5], [6]. Other works convexify the problem by semidefinite programming (SDP) relaxation [7] or second-order cone programming (SOCP) relaxation [8]. For example, in [9], Zhang *et al.* give the sufficient conditions when the SDP relaxation is tight for conducting voltage regulation in distribution grids.

Another research line focuses on the dynamics of voltage control (typically together with frequency control). For example, in [10], Schiffer *et al.* prove that a consensus-based distributed voltage control can uniquely determine the equilibrium point of the closed-loop voltage and reactive power dynamics. For more related works in this vein, see [11] for an excellent review.

Our work falls into the first category. While we also start with designing the distributed control scheme for a simplified linear network model, our major contribution is to devise an analytical framework to show that our scheme gives convergence guarantee in the non-convex branch flow model. To the best of our knowledge, our work is the first attempt to analyze gradient type algorithms derived from linearized branch flow model for AC model.

The remainder of this paper is organized as follows. In Section II, we briefly review the branch flow model and its simplifications (linearization). Then, we investigate the distributed control schemes to conduct voltage regulation using the linearized branch flow model in Section III. In this section, we also highlight the role of communication network on the design. To show the performance of our proposed scheme for the branch flow model, we first analyze the performance of the scheme for the linearized model in Section IV. Based on this analysis, we then show the convergence guarantee for the non-convex model in Section V. We verify the performance of the scheme by simulation in Section VI. Finally, the concluding remarks and future directions are given in Section VII.

C. Wu is with the Institute for Interdisciplinary Information Sciences, Tsinghua University. Email: chenye.wu@tsinghua.edu.cn.

G. Hug are with the Power Systems Laboratory, ETH Zurich, Email: hug@eeh.ee.ethz.ch.

S. Kar is with Department of ECE, Carnegie Mellon University, Pittsburgh, PA 15213, Email: soumyak@andrew.cmu.edu.

II. NETWORK MODEL AND ITS SIMPLIFICATIONS

A. Branch Flow Model

We consider a radial distribution system, represented by a graph $\mathcal{G} = \{\mathcal{N}, \mathcal{E}\}$. \mathcal{N} is the set of nodes, indexed by $i = 0, \dots, n$, where node 0 is the substation. \mathcal{E} stands for the set of distribution lines in the system. The radial structure allows us to conveniently define the direction of distribution lines. For each $(i, j) \in \mathcal{E}$, node j is the parent of node i .

For each line (i, j) , denote its impedance by $z_i = r_i + \mathbf{i}x_i$; let I_i and $S_i = P_i + \mathbf{i}Q_i$ be the complex current and the complex power flowing from node i to j , respectively. At each node $i \in \mathcal{N}$, we denote its complex voltage by V_i , its complex power consumption and generation by $s_i^d = p_i^d + \mathbf{i}q_i^d$, and $s_i^g = p_i^g + \mathbf{i}q_i^g$, respectively.

The branch flow model [12] assumes a given and fixed voltage V_0 at the substation. For notational simplicity, we define $l_i := |I_i|^2$, $v_i := |V_i|^2$. We also denote the child set of node i by $\delta(i)$. These yield [12]:

$$S_i = s_i^g - s_i^d + \sum_{k \in \delta(i)} (S_k - (r_k + \mathbf{i}x_k)l_k), \forall i \in \mathcal{N}, \quad (1)$$

$$v_i = v_j + 2(r_i P_i + x_i Q_i) - (r_i^2 + x_i^2)l_i, \forall (i, j) \in \mathcal{E}, \quad (2)$$

$$l_i v_i = P_i^2 + Q_i^2, \forall i \in \mathcal{N} \setminus \{0\}. \quad (3)$$

Setting $S_0 = 0 + \mathbf{i}0$ enforces the power balance constraint at the substation: $s_0^g - s_0^d$ is the total net power injection into the distribution network from the main grid.

B. Simplified Branch Flow Model

In this paper, we first study the voltage regulation problem in a simplified network model to highlight the structure of the problem. In Section V, we will show the performance of the proposed control scheme for the non-convex branch flow model. We follow [13] and assume that the real and reactive power losses are much smaller than the power flows. This simplifies the branch flow model:

$$S_i = s_i^g - s_i^d + \sum_{k \in \delta(i)} S_k, \forall i \in \mathcal{N}, \quad (4)$$

$$v_i = v_j + 2(r_i P_i + x_i Q_i), \forall (i, j) \in \mathcal{E}. \quad (5)$$

In order to give a better intuition behind the proposed control scheme, we further analyze the structure of the simplified branch flow model. Let us consider a simple line network, as shown in Fig. 1. Suppose all the voltage amplitudes are 1 p.u. at time t :

$$v_i^t = 1 \text{ p.u.}, \text{ and } r_i P_i^t + x_i Q_i^t = 0, \forall i.$$

Suppose there is a disturbance at bus 3, at time $t + 1$:

$$s_3^{d,t+1} = s_3^{d,t} + \Delta P_3 + \mathbf{i}\Delta Q_3.$$

Note that, since the generation and consumption at bus 4 and bus 5 remain the same, S_4 and S_5 remain the same. This is why in Fig. 2, $v_3^{t+1} = v_4^{t+1} = v_5^{t+1}$ using this model.

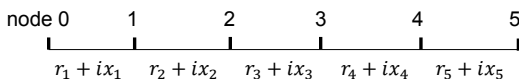


Fig. 1: Illustrative example: line network.

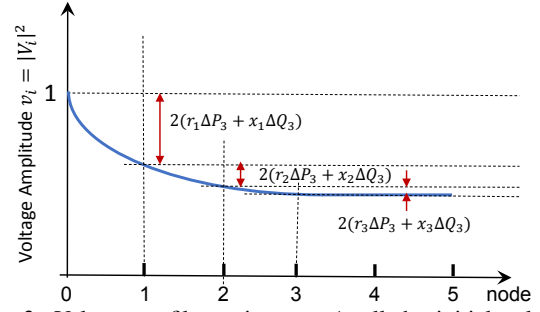


Fig. 2: Voltage profile at time $t + 1$; all the initial voltage amplitudes are 1 p.u.

The sudden disturbance at bus 3 will change the power flows S_1, S_2 , and S_3 . This will in turn change the relationship between the three voltage amplitudes:

$$v_i^{t+1} = v_{i-1}^{t+1} - 2(r_i \Delta P_3 + x_i \Delta Q_3), i = 1, 2, 3. \quad (6)$$

Remark: This simplified model highlights the structure of the problem: when there is a disturbance at a certain node, the power flow in successors of the disturbed node remains unchanged. Thus, the disturbance will have the same effect on the voltage amplitude for the successors while the disturbance will have an ‘escalator’ effect on its ancestors. Fig. 2 visualizes these effects. These effects will later help us explain the required communication topology in designing the distributed control scheme.

III. DISTRIBUTED SCHEME DESIGN

A. Problem Formulation

We conduct the voltage regulation by adjusting the reactive power through the PV inverters. One natural objective function is to minimize the total deviations of voltages from their reference values. Another objective function minimizes the adjusted reactive power to reflect the inverter operation cost. Thus, the optimization problem can be casted as follows:

$$\begin{aligned} \min_{q_i^g} \quad & \sum_{i=1}^n \left(v_i - v_i^{ref} \right)^2 + \beta \sum_{i=1}^n |q_i^g - q_i^{g,ref}| \\ \text{s.t.}, \quad & \underline{q}_i^g \leq q_i^g \leq \bar{q}_i^g, \forall i \in \mathcal{N} \setminus \{0\}, \\ & S_i = s_i^g - s_i^d + \sum_{k \in \delta(i)} S_k, \forall i \in \mathcal{N}, \\ & v_i = v_j + 2(r_i P_i + x_i Q_i), \forall (i, j) \in \mathcal{E}, \end{aligned} \quad (7)$$

where β is the trade-off parameter; v_i^{ref} and $q_i^{g,ref}$ are the reference voltage and the reference (or the initial) reactive power injection at bus i , respectively.

Instead of having the hard box constraints on q_i^g , we introduce the following soft constraint:

$$\begin{aligned} & f_i(q_i^g) \\ &= \begin{cases} \frac{2(\bar{q}_i^g - q_i^{g,ref})}{\pi} \tan\left(\frac{q_i^g - q_i^{g,ref}}{\bar{q}_i^g - q_i^{g,ref}} \cdot \frac{\pi}{2}\right), & \text{if } q_i^g \in [q_i^{g,ref}, \bar{q}_i^g], \\ \frac{2(q_i^g - \underline{q}_i^{g,ref})}{\pi} \tan\left(\frac{q_i^g - \underline{q}_i^{g,ref}}{\underline{q}_i^{g,ref} - \underline{q}_i^g} \cdot \frac{\pi}{2}\right), & \text{if } q_i^g \in (\underline{q}_i^{g,ref}, \underline{q}_i^g), \\ +\infty, & \text{otherwise.} \end{cases} \end{aligned}$$

As shown in Fig. 3, when $q_i^g - q_i^{g,ref}$ is reasonably small,

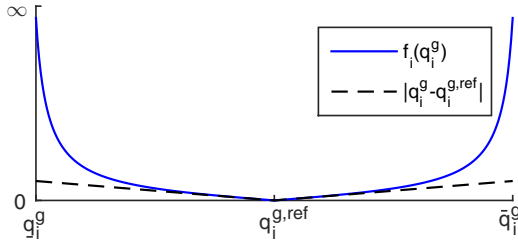


Fig. 3: Visualization of $f_i(q_i^g)$.

$$f(q_i^g) \approx |q_i^g - q_i^{g,ref}|.$$

Thus, we can directly replace the second term in the objective function and ignore the box constraints on q_i^g :

$$\begin{aligned} \min_{q_i^g} \quad & \sum_{i=1}^n (v_i - v_i^{ref})^2 + \beta \sum_{i=1}^n f_i(q_i^g) \\ \text{s.t.}, \quad & S_i = s_i^g - s_i^d + \sum_{k \in \delta(i)} S_k, \forall i \in \mathcal{N}, \\ & v_i = v_j + 2(r_i P_i + x_i Q_i), \forall (i, j) \in \mathcal{E}. \end{aligned} \quad (8)$$

B. Design with Tree Communication Network

Denote the unique path from node 0 to node i by \mathcal{P}_i . Let $0 \notin \mathcal{P}_i$, and $i \in \mathcal{P}_i$. Denote the Lagrangian multiplier associated with the i^{th} voltage constraint in (8) by w_i . The Karush-Kuhn-Tucker (KKT) conditions are given by all the constraints in (8), together with for $i = 1, \dots, n$:

$$2(v_i - v_i^{ref}) - (w_i - \sum_{j \in \delta(i)} w_j) = 0, \quad (9)$$

$$\beta f'_i(q_i^g) - 2(w_i x_i + \sum_{j \in \mathcal{P}_i} w_j x_j) = 0. \quad (10)$$

These conditions allow us to design the following natural distributed voltage regulation scheme (the primal dual decomposition [14]):

Scheme with Tree Communication Network

At each round t , $t = 1, 2, \dots$, do the following:

Phase 1: from leaves to the root, sequentially compute the Lagrangian multipliers:

For node i , after receiving all its child(ren) information, it can compute its own multiplier

$$w_i^t = 2(v_i^t - v_i^{ref}) + \sum_{j \in \delta(i)} w_j^t.$$

It will send its parent its own multiplier as well as all information about its child(ren).

Phase 2: from root to leaves, sequentially exchange the multipliers and conduct the control: for node i , after receiving all its ancestor information, it can conduct the reactive power control for the next round

$$\hat{q}_i^{g,t+1} = f_i^{-1} \left(\frac{2(w_i^t x_i + \sum_{j \in \mathcal{P}_i} w_j^t x_j)}{\beta} \right), \quad (11)$$

$$q_i^{g,t+1} = \hat{q}_i^{g,t+1} + \alpha (\hat{q}_i^{g,t+1} - q_i^{g,t}), \quad (12)$$

where α is the step size. Then, it passes its Lagrangian multiplier to all the nodes in its child set.

Stopping criteria: given tolerance $\eta > 0$,

$$|q_i^{g,t+1} - q_i^{g,t}| < \eta, \quad \forall i \in \mathcal{N}.$$

Remark: Note that after the first phase, no nodes (except the root) know its parent's information (multiplier). This is why we require two sequential processes in the distributed control. Since the optimization problem is strictly convex, this simple iterative distributed scheme is guaranteed to converge as long as a suitable α is selected [14].

C. Design with Complete Communication Network

The distributed control scheme discussed above requires a tree communication network, which has exactly the same structure as the radial distribution network. If we have a different communication network, we may be able to devise a more efficient distributed control scheme.

For example, suppose we have a complete communication network. We can combine the two constraints in (8):

$$v_k = v_0 + \sum_{i=1}^n R_{ki}(p_i^g - p_i^d) + \sum_{i=1}^n X_{ki}(q_i^g - q_i^d), \quad (13)$$

where

$$R_{ki} := 2 \sum_{h \in \mathcal{P}_k \cap \mathcal{P}_i} r_h, \text{ and } X_{ki} := 2 \sum_{h \in \mathcal{P}_k \cap \mathcal{P}_i} x_h.$$

Optimization problem (8) then becomes

$$\begin{aligned} \min_{q_i^g} \quad & \sum_{i=1}^n (v_i - v_i^{ref})^2 + \beta \sum_{i=1}^n f_i(q_i^g) \\ \text{s.t.}, \quad & v_k = v_0 + \sum_{i=1}^n R_{ki}(p_i^g - p_i^d) + \sum_{i=1}^n X_{ki}(q_i^g - q_i^d). \end{aligned} \quad (14)$$

Note that problem (14) is not really a constrained optimization problem. The constraints simply define how v_k 's are functions of $\mathbf{q}^g = (q_1^g, \dots, q_n^g)^T$, i.e., $v_i(\mathbf{q}^g)$. In essence, problem (14) is a unconstrained optimization problem¹. Denote

$$h(\mathbf{q}^g) = \sum_{i=1}^n (v_i(\mathbf{q}^g) - v_i^{ref})^2 + \beta \sum_{i=1}^n f_i(q_i^g). \quad (15)$$

As long as $h(\mathbf{q}^g)$ is convex (which is straightforward to verify), the original optimization problem can be solved by the gradient descent algorithm. The standard gradient descent algorithm will conduct the following update: at round t , for each entity i :

$$q_i^{g,t+1} = q_i^{g,t} - \alpha g_i^t, \quad (16)$$

where

$$g_i^t = \left. \frac{\partial h}{\partial q_i^g} \right|_{q_i^g = q_i^{g,t}} = 2 \sum_{k=1}^n (v_k^t - v_k^{ref}) X_{ki} + \beta f'_i(q_i^{g,t}). \quad (17)$$

This leads to our distributed control scheme with the complete communication network:

Scheme with Complete Communication Network

At each round t , $t = 1, 2, \dots$, do the following:

¹For comparison, Hauswirth *et al.* investigate the convergence of gradient descent algorithm for the constrained optimization problem with the application on solving the optimal AC power flow in an online fashion in [15].

Phase 1: each node i measures the local voltage and computes

$$w_i^t = 2(v_i^t - v_i^{ref}).$$

Then, each node broadcasts the signal to all the other nodes. *Phase 2:* each node will update its own reactive power control signal in a gradient descent way:

$$q_i^{g,t+1} = q_i^{g,t} - \alpha \left(\sum_{k=1}^n w_k^t X_{ki} + \beta f'_i(q_i^{g,t}) \right),$$

where α is the step size.

Stopping criteria: given tolerance $\eta > 0$,

$$|q_i^{g,t+1} - q_i^{g,t}| < \eta, \forall i \in \mathcal{N}.$$

Remark: This is a more efficient distributed control scheme compared to the scheme with the tree structure communication network. In this case, we do not need two rounds of sequential updates. All the nodes can compute the value they need to communicate (local Lagrangian multiplier) by local voltage measurements. By exchanging the Lagrangian multipliers, all the nodes can perform the reactive power control, which will iteratively solve the problem.

Note that the definitions of R_{ki} and X_{ki} highlight the fact that when conducting the distributed control, we need to put more weights on all the ancestors. This is also aligned with the intuition from Section II-B.

IV. PERFORMANCE IN LINEARIZED MODEL

It is not hard to see that optimization problem (14) is convex due to the convex objective function and the linear constraint set. This implies the convergence of the gradient descent algorithm. However, convexity is not enough for us to show the convergence of the proposed algorithm in the non-convex branch flow model. For the subsequent analysis, we will focus the analysis on the complete communication network case. And, we prove that the optimization problem (14) is strongly convex, which implies the geometrically convergence of the gradient descent algorithm. This serves as the basis of the analysis for the general network model.

A. Strong Convexity

Definition 1. A differentiable function f is called strongly convex with parameter $m > 0$ if the following inequality holds for all points x, y in its domain:

$$(\nabla f(x) - \nabla f(y))^T(x - y) \geq m\|x - y\|_2^2, \quad (18)$$

where $\|x\|_2$ is the 2-norm of vector x .

It is straightforward to see that the second term in $h(\mathbf{q}^g)$ is convex due to the convexity of tangent functions. To show the strong convexity of $h(\mathbf{q}^g)$, it suffices to show its first term (for notational simplicity, denoted by $u(\mathbf{q}^g)$) is strongly convex. Let us start with

$$\frac{\partial u}{\partial q_i^g} = \sum_{k=1}^n 2(v_k - v_k^{ref}) \frac{\partial v_k}{\partial q_i^g} = 2 \sum_{k=1}^n (v_k - v_k^{ref}) X_{ki}. \quad (19)$$

Thus,

$$\begin{aligned} & (\nabla u(\mathbf{q}^{g,1}) - \nabla u(\mathbf{q}^{g,2}))^T(\mathbf{q}^{g,1} - \mathbf{q}^{g,2}) \\ &= \sum_{i=1}^n 2 \sum_{k=1}^n (v_k(\mathbf{q}^{g,1}) - v_k(\mathbf{q}^{g,2})) X_{ki} (q_i^{g,1} - q_i^{g,2}) \\ &= \sum_{i=1}^n 2 \sum_{k=1}^n \sum_{j=1}^n X_{kj} X_{ki} (q_j^{g,1} - q_j^{g,2}) (q_i^{g,1} - q_i^{g,2}) \\ &= 2 \sum_{k=1}^n \left(\sum_{i=1}^n \sum_{j=1}^n X_{ki} X_{kj} (q_j^{g,1} - q_j^{g,2}) (q_i^{g,1} - q_i^{g,2}) \right) \\ &= 2 \sum_{k=1}^n \left(\sum_{i=1}^n X_{ki} (q_i^{g,1} - q_i^{g,2}) \right)^2 \geq \gamma \|\mathbf{q}^{g,1} - \mathbf{q}^{g,2}\|_2^2, \end{aligned}$$

where

$$\gamma := 2 \left(\sum_{k=1}^n \min_i X_{ki} \right). \quad (20)$$

Note that, in the branch flow model, we assume the voltage level at the substation is given and fixed. Therefore, if the root 0 has multiple children, they are naturally decoupled by this assumption. This allows us to focus on the case where root 0 has only *one* child. In this case, for all k , $\min_i X_{ki} \geq x_1 > 0$. Thus, $\gamma \geq 2nx_1 > 0$. This yields

$$(\nabla u(\mathbf{q}^{g,1}) - \nabla u(\mathbf{q}^{g,2}))^T(\mathbf{q}^{g,1} - \mathbf{q}^{g,2}) \geq \gamma \|\mathbf{q}^{g,1} - \mathbf{q}^{g,2}\|_2^2$$

Note that the derivative of f_i is not well-defined at $q_i^{g,ref}$. Thus, we define

$$\left. \frac{\partial f_i}{\partial q_i^g} \right|_{q_i^g = q_i^{g,ref}} = 0$$

to make f_i is differentiable everywhere.

Together with the convexity of the second term in $h(\mathbf{q}^g)$, we have the strong convexity of problem (14):

$$(\nabla h(\mathbf{q}^{g,1}) - \nabla h(\mathbf{q}^{g,2}))^T(\mathbf{q}^{g,1} - \mathbf{q}^{g,2}) \geq \gamma \|\mathbf{q}^{g,1} - \mathbf{q}^{g,2}\|_2^2$$

B. Convergence Speed

Theorem 2. The update rule $\mathbf{x}^{t+1} = \mathbf{x}^t - \alpha \mathbf{g}^t$ in the gradient descent algorithm (with step size α) to find the optimum \mathbf{x}^* of strongly convex function $f(\mathbf{x})$ with parameter m , satisfies for any $t = 1, \dots, T$,

$$\|\mathbf{x}^t - \mathbf{x}^*\|_2^2 \leq (1 - 2\alpha m)^{t-1} \|\mathbf{x}^1 - \mathbf{x}^*\|_2^2 + \frac{\alpha}{2m} \max_{1 \leq k \leq t} \|\mathbf{g}^k\|_2^2.$$

In particular, \mathbf{x}^t converges to \mathbf{x}^* geometrically with systematic error $\frac{\alpha}{2m} \max_{1 \leq k \leq t} \|\mathbf{g}^k\|_2^2$.

The proof is given in the Appendix. The geometrical convergence speed allows us to show the performance guarantee in the non-convex branch flow model.

V. PERFORMANCE IN BRANCH FLOW MODEL

In this section, we will prove the convergence guarantee of our proposed distributed control scheme for the non-convex branch flow model. The proof is inspired by [16], and is based on the analysis in the previous section. Again, we focus on the complete communication network case.

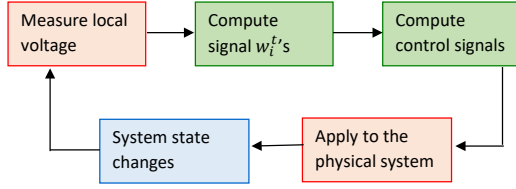


Fig. 4: Distributed control on real system.

As shown in Fig. 4, we will directly employ the gradient descent distributed control. However, note that, after each entity has applied its control action q_i^g , the voltage levels will change according to the physical laws, instead of the branch flow model or the linearized model. Between these two models, the branch flow model is a more accurate representation of the flows and the voltages. However, it defines a non-convex constraint set, which may lead to many local optima. It is a common assumption that the performance of any local optimum and that of the global optimum are very close. Bearing this assumption in mind, in this section, we show that our distributed scheme will converge to some local optimum with bounded error. We will also verify this assumption with simulation.

A. Convergence Guarantee

The most critical challenge in the convergence analysis is that in the branch flow model, the gradient is more complex than that in (17). More importantly, in practice, even the branch flow model is an approximation. That is, if we use the measured voltage to compute the gradient, it is not the gradient for the optimization problem (14).

Denote the true gradient for problem (14) by g^t , and the actually implemented gradient by \hat{g}_i^t , we have

$$\hat{g}^t = g^t + \epsilon^t, \quad (21)$$

where ϵ^t takes into account all the disturbances and can be either positive or negative. With these, we can prove the following theorem (proof is given in the Appendix):

Theorem 3. *The update rule $\mathbf{q}^{t+1} = \mathbf{q}^t - \alpha \hat{g}^t$ satisfies for any $t = 1, \dots, T$,*

$$\begin{aligned} & \|\mathbf{q}^t - \mathbf{q}^*\|_2^2 \\ & \leq (1 - 2\alpha\gamma)^{t-1} \|\mathbf{q}^1 - \mathbf{q}^*\|_2^2 + \frac{1}{\gamma} \max_{1 \leq k \leq t} \|\epsilon^k\| \|\mathbf{q}^k - \mathbf{q}^*\| \\ & \quad + \frac{\alpha}{2\gamma} \max_{1 \leq k \leq t} \|\mathbf{g}^k + \epsilon^k\|_2^2. \end{aligned}$$

In particular, \mathbf{q}^t converges to \mathbf{q}^* (any local optimum) geometrically with systematic error $\frac{1}{\gamma} \max_k \|\epsilon^k\| \|\mathbf{q}^k - \mathbf{q}^*\| + \frac{\alpha}{2\gamma} \max_k \|\mathbf{g}^k + \epsilon^k\|_2^2$.

Remark: The systematic error can be very small. Note that $\gamma \geq 2nx_1$, which grows linearly in the number of nodes. Another important factor in deciding this error is $\|\epsilon^t\|_2$. We use simulations to test its magnitude in the next section. It is worth noting that because we choose to use the tangent barrier function, the magnitude of gradient \mathbf{g} might be very large if the optimum is near the boundary. One way to solve

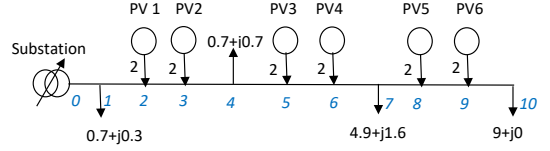


Fig. 5: Test feeder: all parameters are given in p.u.

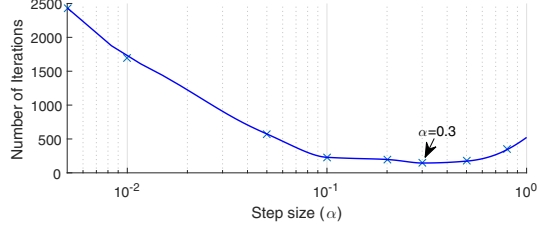


Fig. 6: Impact of step size on convergence speed.

this issue could be to use a vanishing step size sequence $\{\alpha^t\}_{t=1}^\infty$, which satisfies the following two conditions:

$$\sum_{t=1}^\infty \alpha^t = \infty, \quad (22)$$

$$\sum_{t=1}^\infty (\alpha^t)^2 < \infty. \quad (23)$$

VI. SIMULATION RESULTS

To verify the performance of our scheme, we conduct simulations on the prototype IEEE 34-node feeder system, as shown in Fig. 5 (simplified to 11-node system in [4], original system proposed in [17]). We assume that six nodes have the capability of conducting voltage regulation. The capability may come from a large PV farm, or a collection of rooftop PV panels (possibly controlled by a local aggregator). The communication is between all the nodes, since we want to ensure the desired voltage profile across the system. The line characteristics are given in Table I. The reference reactive power generations ($q_i^{g,ref}$ in the formulation, or the initial reactive power generation in practice) at all the six controllable nodes are set to be zero. The box constraints on the q_i^g 's are set to be within $[-3.6, 3.6]$ p.u. We choose 0.001 for parameter β .

In the simulation, we choose the stopping tolerance η to be 0.0001. Figure 6 shows the number of iterations required to converge for different step sizes. It is straightforward to see that a too small step size will inevitably require more iterations to converge. A too large step size, on the other

TABLE I: Line Characteristics ($\times 10^{-3}$ p.u.)

Line	1	2	3	4	5	6	7	8	9	10
r	3.5	4.5	1.5	1	1	3	2.5	2	1.5	1.5
x	7.5	8	2.5	2.5	2	7.5	6	4	3.5	2

TABLE II: Optimal Points Comparison

α	voltage (node)			control action (node)		
	1	5	9	2	5	9
0.05	1.0065	1.0159	0.9817	0.4677	0.6858	1.1956
0.3	1.0068	1.0170	0.9848	0.4401	0.6690	1.2497
0.8	1.0030	1.0103	0.9920	0.0116	0.3406	1.6662

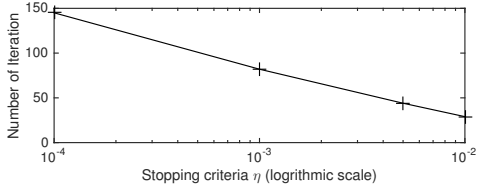


Fig. 7: Verification of the geometrical convergence speed: stopping criteria v.s. iteration numbers

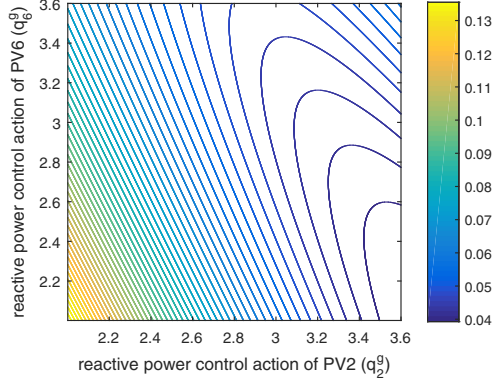


Fig. 8: Contour of the optimization problem with branch flow model.

hand, may cause oscillations around the optimum and hence also require more iterations. In our setting, a step size of 0.3 achieves the minimal iteration number of 145. Figure 7 further verifies that our distributed voltage regulation scheme converges geographically in the stopping tolerance η .

We exemplify the optimal points achieved by different step sizes in Table II. It is interesting to note that although the final voltage profiles are almost identical, the reactive power control profiles (i.e., q_i^g 's) can be quite different. On the one hand, this highlights the non-convexity of the problem when using the branch flow model. On the other hand, this is largely because we choose a very small trade-off parameter β , which means that even with very diverse reactive control profiles, the objective values at different local optima can be very close. We visualize the contour of the optimization problem with branch flow model in Fig. 8 (with only two controllable PV farms, at node 2 and node 6 respectively). The global minimum lies within the dark blue circle in the lower right corner. However, all the points within this circle have very similar objective values. With a sampling rate of 0.01, the difference is at most on the order of 10^{-5} . This is

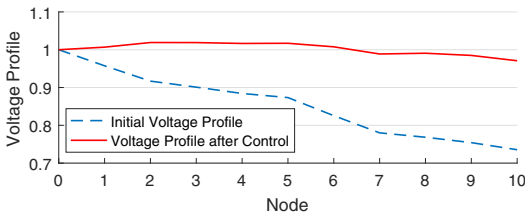


Fig. 9: Voltage profile: initial v.s. after control.

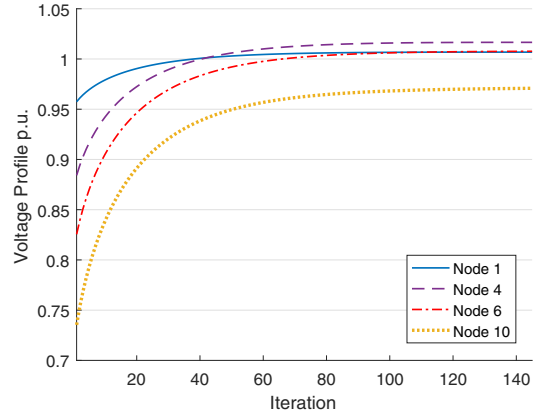


Fig. 10: Voltage profile evolution during iteration.

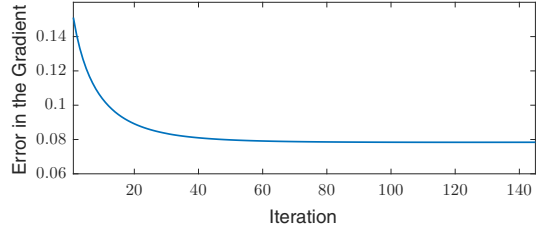


Fig. 11: Gradient error $\|\epsilon^t\|_2$ during iteration.

also true for the points within the other sparsely distributed dark blue circles. In other words, the function is very flat around the global optimum. This implies that many points in these areas can be regarded as the local minimum in our approach. This explains why it is possible that two local minima can have very diverse control actions. It is worth noting that for better visualization, Fig. 8 only shows the contour of the optimization problem with two controllable PV farms. With more PV farms, the optimization problem will become more non-convex, and will not have such a nice structure.

Figure 9 shows the initial voltage profile with no reactive power control by the PV generators and the voltage profile after the application of the distributed control. Obviously, the distributed control scheme pushes the voltage profile to within the limits. Figure 10 further illustrates the voltage profile evolution at selected nodes. There is no obvious oscillations and all the voltages are moving towards their reference values (1 p.u. in our simulation).

We also examine the error between the gradient for problem (14) and the actually implemented gradient, i.e., $\|\epsilon^t\|_2$'s. Figure 11 illustrates that this error approaches a small constant (0.08) after several initial iterations.

VII. CONCLUSIONS

In this paper, we devise a distributed framework to conduct voltage regulation in the distribution network. In the framework, we exploit the reactive power control potential offered by the inverters of the PV panels. We further prove the convergence guarantee of our scheme for the branch flow model and characterize the systematic error (in particular, the gradient error $\|\epsilon^t\|_2$) brought by the non-convexity.

Though promising, much remains unclear. For example, it is not straightforward to extend our scheme to conduct voltage regulation with joint active and reactive power control. Technically, this is more challenging due to the coupling constraints of the real and reactive power. Practically, this is more challenging because we want to exploit the most reasonable cost function for adjusting real power. We plan to include net metering, profits by participating demand response, and the operational cost in the cost function.

Another interesting aspect of the research is the incentive issue. We have focused on the problem from a social planner's perspective and ignore the market design in this paper. A number of recent works (including [18], [19]) illuminate the major opportunities and challenges in designing the market for joint frequency and voltage regulation in the distribution network.

VIII. APPENDIX

A. Proof for Theorem 2

$$\begin{aligned}
\|\mathbf{x}^{t+1} - \mathbf{x}^*\|_2^2 &= \|\mathbf{x}^t - \alpha \mathbf{g}^t - \mathbf{x}^*\|_2^2 \\
&= \|\mathbf{x}^t - \mathbf{x}^*\|_2^2 - 2\alpha(\mathbf{g}^t)^T(\mathbf{x}^t - \mathbf{x}^*) + \alpha^2\|\mathbf{x}^t\|_2^2 \\
&\leq \|\mathbf{x}^t - \mathbf{x}^*\|_2^2 - 2\alpha m\|\mathbf{x}^t - \mathbf{x}^*\|_2^2 + \alpha^2\|\mathbf{g}^t\|_2^2 \\
&\leq (1 - 2\alpha m)^t\|\mathbf{x}^1 - \mathbf{x}^*\|_2^2 \\
&\quad + \alpha(1 - (1 - 2\alpha m)^t)/2m \max_{1 \leq k \leq t} \|\mathbf{g}^k\|_2^2 \\
&\leq (1 - 2\alpha m)^t\|\mathbf{x}^1 - \mathbf{x}^*\|_2^2 + \alpha/2m \max_{1 \leq k \leq t} \|\mathbf{g}^k\|_2^2.
\end{aligned} \tag{24}$$

The first inequality utilizes the fact that $f(\mathbf{x})$ is strictly convex, with parameter m . The last two inequalities are standard manipulations.

B. Proof for Theorem 3

This proof aligns with that of Theorem 2.

$$\begin{aligned}
\|\mathbf{q}^{t+1} - \mathbf{q}^*\|_2^2 &= \|\mathbf{q}^t - \alpha \hat{\mathbf{g}}^t - \mathbf{q}^*\|_2^2 \\
&= \|\mathbf{q}^t - \alpha(\mathbf{g}^t + \epsilon^t) - \mathbf{q}^*\|_2^2 \\
&= \|\mathbf{q}^t - \mathbf{q}^*\|_2^2 - 2\alpha(\mathbf{g}^t + \epsilon^t)^T(\mathbf{q}^t - \mathbf{q}^*) + \alpha^2\|\mathbf{g}^t + \epsilon^t\|_2^2 \\
&\leq \|\mathbf{q}^t - \mathbf{q}^*\|_2^2 - 2\alpha\gamma\|\mathbf{q}^t - \mathbf{q}^*\|_2^2 \\
&\quad - 2\alpha(\epsilon^t)^T(\mathbf{q}^t - \mathbf{q}^*) + \alpha^2\|\mathbf{g}^t + \epsilon^t\|_2^2 \\
&\leq (1 - 2\gamma\alpha)^t\|\mathbf{q}^1 - \mathbf{q}^*\|_2^2 \\
&\quad + (1 - (1 - 2\gamma\alpha)^t)/\gamma \max_{1 \leq k \leq t} |(\epsilon^k)^T(\mathbf{q}^k - \mathbf{q}^*)| \\
&\quad + \alpha(1 - (1 - 2\gamma\alpha)^t)/2\gamma \max_{1 \leq k \leq t} \|\mathbf{g}^k + \epsilon^k\|_2^2 \\
&\leq (1 - 2\gamma\alpha)^t\|\mathbf{q}^1 - \mathbf{q}^*\|_2^2 + 1/\gamma \max_{1 \leq k \leq t} \|\epsilon^k\|_2\|\mathbf{q}^k - \mathbf{q}^*\|_2 \\
&\quad + \alpha/2\gamma \max_{1 \leq k \leq t} \|\mathbf{g}^k + \epsilon^k\|_2^2.
\end{aligned} \tag{25}$$

Again, the first inequality utilizes the fact that $h(\mathbf{q})$ is strictly convex. The last inequality uses the Cauchy-Schwarz inequality.

REFERENCES

- [1] R. Beveridge and K. Kern, "The Energiewende in Germany: Background, Developments and Future Challenges," *Renewable Energy Law and Policy Review*, p. 3, 2013.
- [2] R. Yan and T. K. Saha, "Investigation of voltage stability for residential customers due to high photovoltaic penetrations," *IEEE Transactions on Power Systems*, vol. 27, no. 2, pp. 651–662, May 2012.
- [3] M. E. Baran and I. M. El-Markabi, "A multiagent-based dispatching scheme for distributed generators for voltage support on distribution feeders," *IEEE Transactions on Power Systems*, vol. 22, no. 1, pp. 52–59, Feb 2007.
- [4] K. Turitsyn, P. ulc, S. Backhaus, and M. Chertkov, "Distributed control of reactive power flow in a radial distribution circuit with high photovoltaic penetration," in *IEEE PES General Meeting*, July 2010, pp. 1–6.
- [5] S. Bolognani, R. Carli, G. Cavraro, and S. Zampieri, "Distributed reactive power feedback control for voltage regulation and loss minimization," *IEEE Transactions on Automatic Control*, vol. 60, no. 4, pp. 966–981, April 2015.
- [6] J. Lavaei and S. H. Low, "Zero duality gap in optimal power flow problem," *IEEE Transactions on Power Systems*, vol. 27, no. 1, pp. 92–107, 2012.
- [7] L. Gan, N. Li, U. Topcu, and S. H. Low, "Exact convex relaxation of optimal power flow in radial networks," *IEEE Transactions on Automatic Control*, vol. 60, no. 1, pp. 72–87, 2015.
- [8] B. Zhang, A. Y. S. Lam, A. D. Dominguez-Garcia, and D. Tse, "An optimal and distributed method for voltage regulation in power distribution systems," *IEEE Transactions on Power Systems*, vol. 30, no. 4, pp. 1714–1726, July 2015.
- [9] J. Schiffer, T. Seel, J. Raisch, and T. Sezi, "Voltage stability and reactive power sharing in inverter-based microgrids with consensus-based distributed voltage control," *IEEE Transactions on Control Systems Technology*, vol. 24, no. 1, pp. 96–109, Jan 2016.
- [10] J. Schiffer, D. Zonetti, R. Ortega, A. M. Stankovic, T. Sezi, and J. Raisch, "Modeling of microgrids - from fundamental physics to phasors and voltage sources," *CoRR*, vol. abs/1505.00136, 2015. [Online]. Available: <http://arxiv.org/abs/1505.00136>
- [11] M. Baran and F. F. Wu, "Optimal sizing of capacitors placed on a radial distribution system," *IEEE Transactions on Power Delivery*, vol. 4, no. 1, pp. 735–743, Jan 1989.
- [12] M. E. Baran and F. F. Wu, "Network reconfiguration in distribution systems for loss reduction and load balancing," *IEEE Transactions on Power Delivery*, vol. 4, no. 2, pp. 1401–1407, 1989.
- [13] S. Boyd and L. Vandenberghe, *Convex optimization*. Cambridge university press, 2004.
- [14] A. Hauswirth, S. Bolognani, F. Dörfler, and G. Hug, "Projected gradient descent on riemannian manifolds with applications to online power system optimization," in *54th Annual Allerton Conference on Communication, Control, and Computing*, Sept 2016.
- [15] S. Arora, R. Ge, T. Ma, and A. Moitra, "Simple, efficient, and neural algorithms for sparse coding," *arXiv preprint arXiv:1503.00778*, 2015.
- [16] W. Kersting, "Radial Test Feeders." [Online]. Available: <http://ewh.ieee.org/soc/pes/dsacom/testfeeders.html>
- [17] C. Wu, H. Mohsenian-Rad, and J. Huang, "Pev-based reactive power compensation for wind dg units: A stackelberg game approach," in *Proc. of IEEE SmartGridComm 2012*. IEEE, 2012, pp. 504–509.
- [18] N. Li, "A market mechanism for electric distribution networks," in *Proc. of IEEE CDC 2015*, Dec 2015, pp. 2276–2282.